

2-Thiobenzyl-6-Methylbenzoxazole As An Effective Copper Corrosion Inhibitor In 2M HNO₃: Experimental And DFT Studies

Ehouman A. D¹, Diomandé G.G.D²., Niamien P. M.
¹, Sissouma D. ², Trokourey A¹.

¹Laboratoire de Chimie Physique, UFHB Cocody-Abidjan

²Laboratoire de Chimie Organique Structurale, UFHB, Cocody-Abidjan

Abstract: 2-Thiobenzyl-6-Methylbenzoxazole (2-TB6MBXA) has been tested as an inhibitor of copper corrosion in 2M HNO₃, using mass loss method and a quantum chemical method based on DFT (B3LYP/6-31G (d)). The results show that this molecule is a good inhibitor. 2-TB6MBXA adsorbs on copper according to Langmuir modified adsorption isotherm. The thermodynamic adsorption and activation parameters indicate a chemisorption process and an endothermic dissolution process. The molecular and chemical reactivity descriptors (global and local) confirm the experimental data.

Keywords: Copper, corrosion inhibition, DFT, mass loss, nitric acid, 2-Thiobenzyl-6-Methylbenzoxazole

I. Introduction

Copper and its alloys [1] are often used in many applications in modern chemistry. Copper is a relatively noble metal, however, it undergoes corrosion when being in contact with acidic solutions, especially in the presence of oxygen or other oxidants. The behavior of copper and its alloys in acidic media is extensively reported in the literature [2, 3] but several schemes have been presented for their dissolution. Organic heterocyclic compounds [4-6] have been reported to be effective inhibitors for copper acid corrosion. The nature of the corrosive inhibitor depends on the material being protected and on the corrosive agent to neutralize. Heterocyclic compounds [7] are employed as corrosion inhibitors because the presence of many adsorption centers (O, N, S, P, and π electrons) helps them to form complexes with metal ions. These complexes constitute a film barrier which separates the metal from the aggressive environment.

In order to support experimental studies, quantum chemical methods are used to provide a molecular level understanding of the observed experimental behavior. The most used of quantum chemical methods for corrosion inhibitor evaluation [8-10] is density functional theory (DFT). This method [11, 12] leads to the ground state properties of a many-electron system by using functionals, i. e. functions of another function, which in this case is the spatially dependent electron density. Nowadays, quantum chemical calculations [13] are widely used to study reaction mechanisms and to interpret the experimental results. To get insight into chemical reactivity and selectivity of organic molecules, researchers use DFT new parameters including global parameters such as electronegativity χ [14], hardness η [15], softness S [16], electrophilicity index ω [17] and local parameters as condensed Fukui functions $f(r)$ [18] and condensed local softness $s(r)$ [19]. The objective of the present paper is to evaluate the behavior of 2-Thiobenzyl-6-methylbenzoxazole against copper corrosion in 2 M HNO₃, by analyzing both experimental data and theoretical parameters.

II. Material and methods

1.1 Copper specimen

The copper specimens were in the form of rod measuring 10 mm in length and 2.2 mm in diameter; they were cut in commercial copper of purity 95% .

2.2 The studied molecule

The molecule of 2-Thiobenzyl-6-methylbenzoxazole (2-TB6MBXA) of brown color has been synthesized in the laboratory. Its molecular structure has been identified by ¹H NMR spectroscopy and mass spectroscopy.

RMN¹H (DMSO-d₆, δ ppm): 2, 93 (3H, s, CH₃); 4, 6 (2H, s, SCH₂); 7, 1-7, 5 (9H, m, H_{ar}).

SDM: m/e (%) = 65 (12%); 91 (100%); 255(25%).

Fig. 1 gives the optimized chemical structure of 2-TB6MBXA.

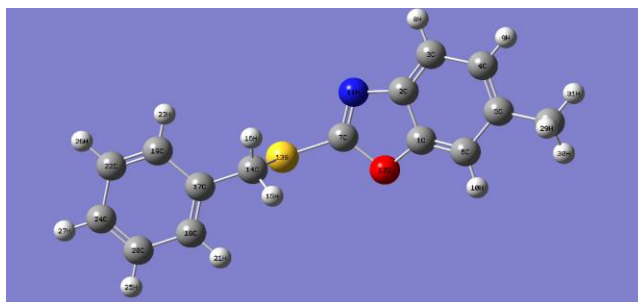


Fig.1: Optimized structure of 2- Thiobenzyl-6-methylbenzoxazole by B3LYP/6-31G (d).

2.3 Solutions

Analytical grade, 65% nitric acid solution from Merck was used to prepare the corrosive aqueous solution. The solution was obtained by dilution of the commercial nitric acid solution using distilled water. The blank was a 2 M HNO₃ solution. The concentrations of the solutions containing (2-TB6MBXA) range from 0.01 to 0.5 mM.

2.4 Mass loss method

The samples were used for mass loss measurements. Prior to all measurements, the specimens were mechanically abraded with different grade emery papers. The specimens were washed thoroughly with distilled water, degreased and rinsed with acetone and dried in a desiccator. Mass loss measurements were carried out in a beaker of 100 mL capacity containing 50 mL of the test solution. The immersion time for mass loss was 1h at a given temperature. In order to get good reproducibility, parallel triplicate experiments were performed and the average mass loss was used to calculate the corrosion rate and the inhibition efficiency using the following equations:

$$W = \frac{\Delta m}{St} \quad (1)$$

$$IE(\%) = \frac{W_0 - W}{W_0} \times 100 \quad (2)$$

2.5 Computational details

Density functional theory (DFT) calculations were carried out using the Becke three-parameter non local exchanged functional [20] with the non-local correlation of Lee et al. [21] and Miehlich et al. [22], together with the standard double zeta plus polarization 6-31 G (d) basis set [23] implemented in Gaussian 03 program package [24]. This method is referred as B3LYP/6-31 G (d) in the standard nomenclature. The geometry of the studied molecule was optimized without symmetry constraints. The following quantum chemical indices were considered: the energy of the highest occupied molecular orbital (E_{HOMO}), the energy of the lowest unoccupied molecular orbital (E_{LUMO}), the energy gap ΔE , the dipole moment (μ) and total energy (E_{T}).

III. Results And Discussion

3.1 Mass loss measurements

3.1.1 Effect of concentration and temperature

The corrosion of copper in 2M HNO₃, at different temperatures (308-328 K) without and with different concentrations in 2-TB6MBXA was investigated. Fig.2 and Fig.3 show, respectively the evolution of the corrosion rate and the inhibition efficiency versus temperature.

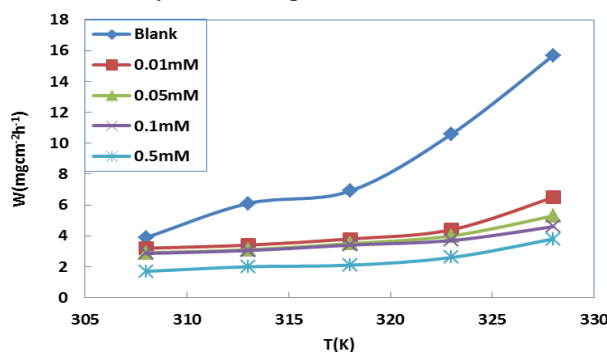


Fig.2: Evolution of corrosion rate of 2-TB6MBXA versus temperature

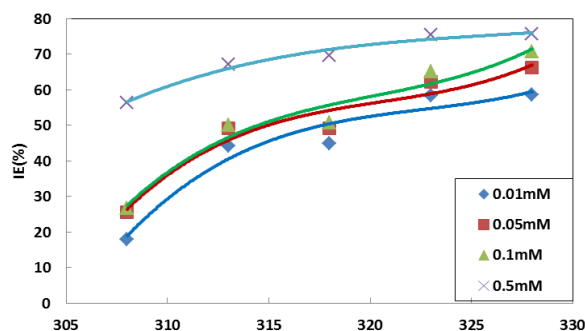
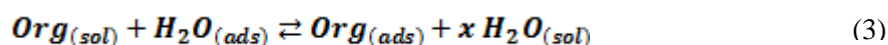


Fig.3: Inhibition efficiency of 2-TB6BMXA versus temperature

Fig.2 shows that for all the concentration studied, the corrosion rate increases with increasing temperature, but it decreases with the increase in 2-TB6MBXA concentration. It is evident from this figure that the rate of corrosion depends on the magnitude of the concentration of the considered molecule. On fig. 3, one can see that the inhibition efficiency grows with an increase in the concentration of the inhibitor. These results could be interpreted as the formation of a film barrier which isolates the metal from its aggressive environment.

3.1.2 Adsorption isotherm

The adsorption isotherm provides information between the inhibitor molecule and the metal surface [25]. This adsorption [26] is regarded as a substitution process between the organic inhibitor in aqueous phase and the water molecules on the metal surface:



Where, $Org_{(sol)}$, $Org_{(ads)}$, $H_2O_{(sol)}$ and $H_2O_{(ads)}$ are respectively the organic molecule and the water molecule in the solution and adsorbed on the metal surface.

Experimental values obtained from mass loss measurements were investigated graphically for fitting several kinds of isotherms, including Langmuir, Temkin, Freundlich and El-Awady. Among these isotherms, excellent fitting of the experimental values has been observed in the Langmuir adsorption isotherm model. According to this adsorption isotherm, the degree of surface coverage θ ($\theta = IE(\%)/100$) [27] is related to the concentration of the inhibitor (C_{inh}) by the following equation:

$$\frac{C_{inh}}{\theta} = \frac{1}{K_{ads}} + C_{inh} \quad (4)$$

Where, K_{ads} stands for the equilibrium constant in the adsorption process. A linear relationship between C_{inh}/θ versus C_{inh} (Fig.4) has been observed with coefficient correlation near unity.

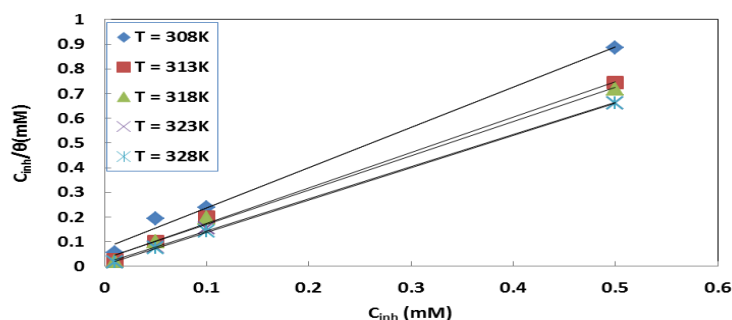


Fig.4: Langmuir adsorption isotherm for 2-TB6-MBXA on copper in 2M HNO₃

Though the correlation coefficient is very strong ($R^2 > 0.998$), we note a deviation of the slopes from unity, showing the existence of interactions between the adsorbed species and therefore that the Langmuir adsorption isotherm can't be applied rigorously. Therefore, the modified Langmuir adsorption isotherm [28], given by the following equation can be applied:

$$\frac{C_{inh}}{\theta} = \frac{n}{K_{ads}} + n C_{inh} \quad (5)$$

The change in standard free adsorption enthalpy was calculated using the equation below:

$$\Delta G_{ads}^0 = -RT \ln(K_{ads} \times 55.5) \quad (6)$$

55.5 is the molar concentration of water in the solution in mol.L⁻¹; *R* is the perfect gas constant and *T* is the absolute temperature.

The changes in adsorption enthalpy and entropy were obtained using the following equation:

$$\Delta G_{ads}^0 = \Delta H_{ads}^0 - T \Delta S_{ads}^0 \quad (7)$$

The plot of ΔG_{ads}^0 versus *T* (Fig.5) leads to the values of ΔH_{ads}^0 and ΔS_{ads}^0

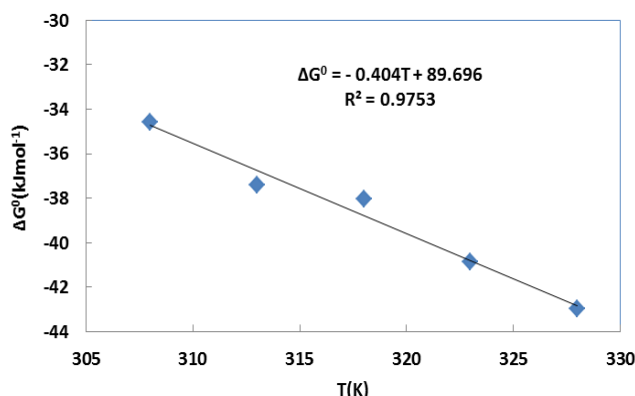


Fig. 5: Change in adsorption free enthalpy versus temperature.

The adsorption parameters are listed in table1.

Table 1: Parameters of the adsorption of 2-TB6MBXA on copper in 2M HNO₃

T(K)	K _{ads} (× 10 ³ M ⁻¹)	ΔG _{ads} ⁰ (kj mol ⁻¹)	ΔH _{ads} ⁰ (kj mol ⁻¹)	ΔS _{ads} ⁰ (J mol ⁻¹ K ⁻¹)
308	13.316	-34.59	89.70	404
313	31.949	-37.42		
318	32.154	-38.04		
323	73.529	-40.86		
328	126.582	-42.97		

In general [29], when ΔG_{ads}^0 values are in the order of -20 kJ mol⁻¹ or even more positive, they are consistent in proving spontaneous adsorption at the interface of charged organic compounds and charged metal surface (physisorption); on the other hand, the values of ΔG_{ads}^0 around -40 kJ mol⁻¹ or more negative involves spontaneous adsorption with charge transfer from the organic inhibitor molecule to the metal (copper) surface via coordination bond formation (chemisorption). In our case, the values of the change in the free enthalpy change range from -42.97 to -34.59 kJ mol⁻¹, showing the predominance of chemisorption. The change in enthalpy ΔH_{ads}^0 is positive, confirming, the chemisorption adsorption process. For the change in entropy ΔS_{ads}^0 , its positive sign indicates an increase in disorder when the adsorption takes place, probably due to the desorption of the water molecules.

3.1.3 Thermodynamic activation parameters

The influence of temperature on the kinetic process of corrosion in free and in the presence of the inhibitor gives information on the behavior of copper/HNO₃ interface. The Arrhenius law was used to determine the apparent energy *E_a* by plotting log*W* versus 1/*T* according to the following equation:

$$\log W = -\frac{E_a}{2.303RT} + \log A \quad (8)$$

Where, *E_a* is the apparent activation energy, *R* is the universal gas constant, *T* is the absolute temperature and *A* is the preexponential factor. The linear regression plot of log*W* versus 1/*T* is given in Fig.6.

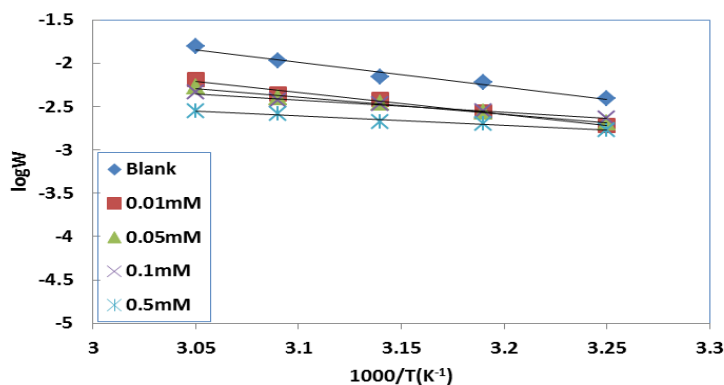


Fig.6 : Arrhenius plots of copper corrosion in 2M HNO₃ without and with 2-TB6MBXA

The changes in activation enthalpy and entropy were calculated using the Eiring transition state equation:

$$\log\left(\frac{W}{T}\right) = \left[\log\frac{R}{Nh} + \frac{\Delta S_a^*}{2.303R} \right] - \frac{\Delta H_a^*}{2.303RT} \quad (9)$$

Where, *h* is the Planck's constant, *N* is the Avogadro number, *T* is the absolute temperature and *R* is the perfect gas constant. Fig.6 depicts the plots of $\log\left(\frac{W}{T}\right)$ versus $\frac{1}{T}$. ΔH_a^* and ΔS_a^* are respectively calculated using the slope ($-\Delta H_a^*/2.303R$) and the intercept $\left[\log\frac{R}{Nh} + \frac{\Delta S_a^*}{2.303R} \right]$. Fig.7 gives the plots of $\log\left(\frac{W}{T}\right)$ versus $1/T$

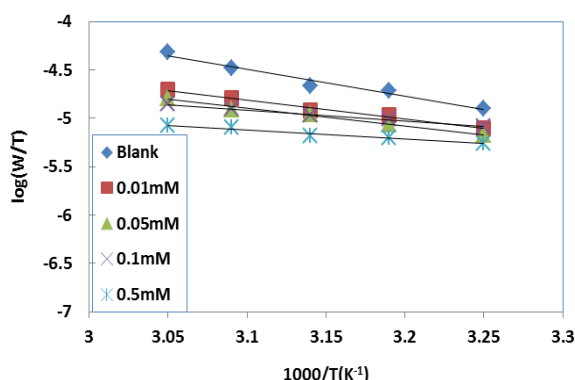


Fig.7: Transition states plots for different concentrations in 2-TB6MBXA

All the activation parameters are listed in table 2.

Table 2: Copper dissolution parameters in 2M HNO₃

Concentration (mM)	$E_a(kJmol^{-1})$	$\Delta H_a^*(kJmol^{-1})$	$\Delta S_a^*(Jmol^{-1}K^{-1})$
0	55.2	52.5	-120.7
0.01	48.5	37.1	-174.3
0.05	37.7	35.1	-182.3
0.1	27.3	22.1	-222.6
0.5	20.6	18.5	-237.8

It is evident from table 2 that the activation energy of the blank is higher than that of inhibited solutions. The activation energy decreases with the increase in the inhibitor concentration. This behavior is consistent with the chemisorption process and it could be explained [30] by a greater coverage due to the formation of a film of copper-inhibitor complex. The positive sign of change in activation enthalpy indicates an endothermic dissolution process and therefore a slow dissolution of copper [31] in the presence of the inhibitor. The change in entropy is negative and it decreases more negatively to a great extent when the inhibitor concentration increases; this behavior [32] reflects the formation on the copper of a stable layer controlled by the inhibitor.

3.2 Quantum chemical studies

DFT calculations have been done to determine the molecular descriptors of the studied molecule. So, the descriptors as E_{HOMO} , the highest occupied molecular orbital, E_{LUMO} , the lowest unoccupied molecular orbital, the HOMO-LUMO energy gap, the dipole moment μ . The reactivity descriptors, including ionization energy (I), chemical affinity (A), electronegativity (χ), hardness (η), softness (S), the fraction (ΔN) of electron transferred and the electrophilicity index (ω) were derived from the molecular descriptors.

According to Koopman's theorem [33], the ionization potential I can be approximated as the negative of the highest occupied molecular orbital (HOMO) energy:

$$I = -E_{\text{HOMO}} \quad (10)$$

The negative of the lowest unoccupied molecular orbital (LUMO) energy is related to the electron affinity A :

$$A = -E_{\text{LUMO}} \quad (11)$$

The electronegativity [34] was obtained using the ionization energy I and the electron affinity A as follows:

$$\chi = \frac{I + A}{2} \quad (12)$$

The hardness which is the reciprocal of the electronegativity was obtained by:

$$\eta = \frac{I - A}{2} \quad (13)$$

When the organic molecule is in contact with the metal, electrons flow from the system with lower electronegativity to that of higher electronegativity until the chemical potential becomes equal. The fraction of electrons transferred, ΔN , was estimated according to Pearson [35]:

$$\Delta N = \frac{\chi_{\text{Cu}} - \chi_{\text{inh}}}{2(\eta_{\text{Cu}} + \eta_{\text{inh}})} \quad (14)$$

In our work, we used theoretical values of χ_{Cu} and η_{Cu} ($\chi_{\text{Cu}} = 4.98$ eV [36] and $\eta_{\text{Cu}} = 0$ [37]).

The global electrophilicity index, introduced by Parr [36] is given by the relation below:

$$\omega = \frac{\chi^2}{2\eta} \quad (15)$$

The molecular and reactivity parameters are listed in table 3.

Table 3: Molecular and reactivity descriptors of 2-TB6MBXA

Descriptor	Value	Descriptor	Value
E_{HOMO} (eV)	-5.734	χ (eV)	3.146
E_{LUMO} (eV)	-0.559	η (eV)	2.587
ΔE (eV)	5.175	S (eV) ⁻¹	0.386
μ (D)	3.045	ΔN	0.354
I (eV)	5.734	ω (eV)	1.913
A (eV)	0.559	E_N (a. u.)	-1107.6

3.2.1 Global reactivity

Table 3 presents the values of the quantum chemical molecular and reactivity parameters of 2-TB6MBXA. The energies [37] of the frontier orbitals E_{HOMO} (energy of the highest occupy molecular orbital) and E_{LUMO} (energy of the lowest unoccupied molecular orbital) are important in defining the reactivity of a chemical compound. E_{HOMO} is often associated with the electron donating ability of a molecule whereas E_{LUMO} indicates the ability of a molecule to accept electrons. Therefore, a high value of E_{HOMO} and a low value of E_{LUMO} suggest efficient adsorption process. The values obtained in our work ($E_{\text{HOMO}} = -5.734$ eV and $E_{\text{LUMO}} = -0.559$ eV) are comparable to that obtained for adsorption inhibitors in the literature [38]. The energy gap ΔE is another parameter that correlates with the reactivity of the organic molecules. Generally, the lower the energy gap, the better the electron transfer process. In this work, the obtained value ($\Delta E = 5.175$ eV) is comparable to many values obtained for many good inhibitors in the literature. The dipole moment μ is another significant parameter which can be used to evaluate the performance of an organic inhibitor; according to many authors [39], a low value of dipole moment favors accumulation of the inhibitor molecules in the surface layer and therefore higher inhibition efficiency. The dipole moment of 2-TB6MBXA ($\mu = 3.045$ D) can be considered [40] as a low value when compared with that of many other molecules.

The ionization potential (I) and the electronic affinity (A) are respectively (5.734 eV) and (0.559 eV). This low value of (I) and the high value of electron affinity indicate the capacity of the molecule both to donate and accept electron. The electronegativity (χ) indicates the capacity of a system to attract electrons, whereas the hardness (η) expresses the degree of reactivity of the system (low values of hardness indicate a tendency to donate electrons). In our work the low value of the electronegativity of the studied molecule when compared to that of copper and the low value of hardness (2.587 eV) confirm the relatively higher value of the fraction of electrons transferred ($\Delta N = 0.354$). The electrophilicity index measures the propensity of chemical species to accept electrons; a high value of electrophilicity index describes a good electrophile while a small value of electrophilicity index describes a good nucleophile. In this work the obtained value ($\omega = 1.913$ eV) shows the good capacity of 2-TB2MBXA to accept electrons.

3.2.2 Local reactivity

The Fukui functions were used to analyze the local reactivity of 2-TB6MBXA as an inhibitor for the corrosion of copper. The condensed Fukui functions and condensed local softness are parameters which enable us to distinguish each part of the molecule on the basis of its chemical behavior due to different substituent functional groups. The Fukui function is defined as:

$$f(\mathbf{r}) = \left(\frac{\partial \rho(\mathbf{r})}{\partial N} \right)_{v(\mathbf{r})} \quad (16)$$

Where $\rho(\mathbf{r})$ is the electron density, N is the number of electrons and $v(\mathbf{r})$ is the external potential, acting on an electron (due in the first instance to atomic nuclei). The regions in a molecule [36] where the Fukui function is large are chemically softer than regions where the function is small. So, invoking the HSAB principle in a local sense, one can establish the behavior of different sites with respect to "hard and soft reagents". Using finite difference approximation, the Fukui function [41] can be defined as:

$$f^+(\mathbf{r}) = \rho_{N+1}(\mathbf{r}) - \rho_N(\mathbf{r}) \quad (17)$$

$$f^-(\mathbf{r}) = \rho_N(\mathbf{r}) - \rho_{N-1}(\mathbf{r}) \quad (18)$$

Where $\rho_N(\mathbf{r})$ is the electron density at a point r in the space around the molecule. N is the number of electrons in the neutral species, when ($N+1$) corresponds to an anion (an electron added to the LUMO of the molecule) and ($N-1$) is the cation (an electron removed from the HOMO of the molecule). The Fukui functions can be condensed to the nuclei by using an atomic charge partitioning scheme, such as the Mulliken population analysis:

$$f_k^+ = q_k(N+1) - q_k(N) \quad (19)$$

$$f_k^- = q_k(N) - q_k(N-1) \quad (20)$$

Where $q(N+1)$, $q(N)$, $q(N-1)$ are Mulliken charge of the atom with ($N+1$), N and ($N-1$) electrons. Fig. 8 gives the HOMO and LUMO densities of the studied molecule. The local softness S_k^+ and S_k^- are given below:

$$S_k^+ = f_k^+ S \quad (21)$$

$$S_k^- = f_k^- S \quad (22)$$

Where S is the global softness. Table 4 gives the values of f_k^+ and f_k^- for 2-TB6MBXA.

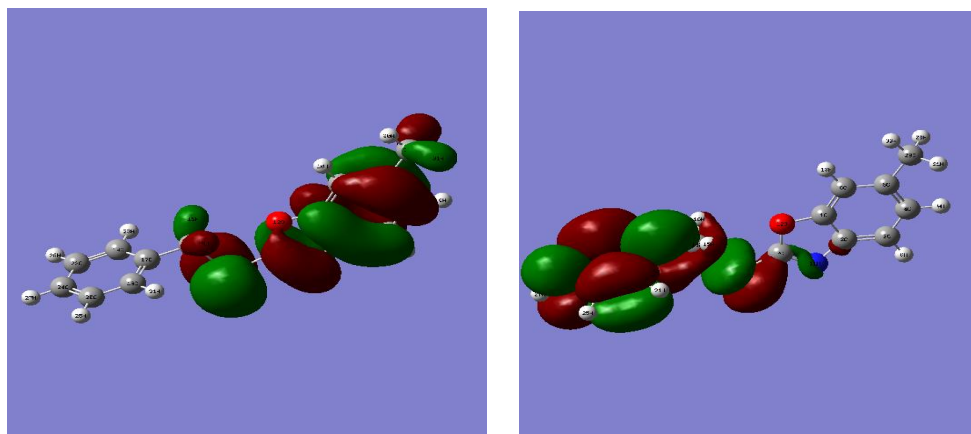


Fig. 8: HOMO (left) and LUMO (right) densities of 2-TB6MBXA

Table 4: Values of Fukui functions and local softness of 2-TB6MBXA

Atom	$q_k(N+1)$	$q_k(N)$	$q_k(N-1)$	f_k^+	f_k^-	S_k^+	S_k^-
3C	-0.250859	-0.166296	-0.151740	-0.084563	-0.014556	-0.032641	-0.005619
4C	-0.209131	-0.191314	-0.179931	-0.017817	-0.011383	-0.006877	-0.004394
6C	-0.237796	-0.237796	-0.213524	-0.058985	-0.024272	-0.022768	-0.009369
7C	0.191492	0.314306	0.273949	-0.122814	0.040357	-0.047406	0.015578
11N	-0.502855	-0.502855	-0.392540	-0.018052	-0.110315	-0.006968	-0.042581
12O	-0.546500	-0.501158	-0.475370	-0.045342	-0.025788	-0.017502	-0.009954
13S	0.013746	0.199709	0.307610	-0.155963	-0.107901	-0.060202	-0.041650
14C	-0.473469	-0.504377	-0.520188	0.030908	0.015811	0.011930	0.006103
18C	-0.192240	-0.161208	-0.163006	-0.031032	0.001798	-0.011978	0.000694
19C	-0.151173	-0.161144	-0.127796	0.009971	-0.033348	0.003849	-0.012872
20C	-0.135807	-0.128519	-0.109731	-0.007288	-0.018788	-0.002813	-0.007252
22C	-0.143726	-0.128531	-0.127149	-0.015195	-0.001382	-0.005865	-0.000533
24C	-0.153164	-0.125812	-0.104264	-0.027352	-0.021548	-0.010558	-0.008317
28C	-0.515804	-0.530704	-0.522424	0.014900	-0.008280	0.005751	-0.003196

From table 4, one can observe that the main adsorption centers of 2TB6MBXA are N (11), O (12), C (14) and C (28). It is also clear that C (7) (in HOMO region) which has the largest value of f_k^- is the probable electrophilic attack center while C (14) (in LUMO region) with the largest value of f_k^+ is the probable nucleophilic attack center.

IV. Conclusion

From the results and findings of the study, the following conclusions can be drawn:

1. The results obtained from gravimetric method indicate that 2-Thiobenzyl-6-Methylbenzoxazole is a good inhibitor for copper corrosion in 2M HNO₃;
2. The inhibition efficiency of 2-TB6MBXA is concentration and temperature dependent;
3. 2-TB6MBXA adsorbs on copper according to Langmuir modified adsorption isotherm;
4. The adsorption of 2-TB6MBXA on copper is spontaneous, endothermic and is consistent with chemisorption.
5. There is a good correlation between quantum chemical (molecular and reactivity) parameters and experimental data.

Acknowledgements

The authors are grateful to the Laboratories of physical chemistry and structural organic chemistry of Houphouet Boigny University of Cocody-Abidjan.

References

- [1] Ph. Marcus, ed., Corrosion Mechanisms in Theory and Practice, 3rd Ed., CRC Press, 2011.
- [2] Yu. I. Kuznetsov, M. O. Agafonkina, H. S. Shikhaliev, N. P. Andeeva, and A. Yu. Potapov, Adsorption passivation of copper by triazoles in neutral aqueous solution, J. Corros. Scale Inhib., 3 (2), 2014, 137-148.
- [3] H. Wang, Q. Wu, C. m. Li, and N. Gu, Copper corrosion inhibition by polyaspartic acid and imidazole, Mater. Corros., 64 (4), 2013, 347-352.
- [4] D. Zhang, L. Gao, and G. Zhou, Inhibition of copper corrosion in aerated hydrochloric acid solution by heterocyclic compounds containing a mercapto group, Corrosion Science, 46(12), 2004, 3031-3040.
- [5] M.A. Elmorsi and A.M. Hassanein, Corrosion inhibition of copper by heterocyclic compounds, Corrosion Science, 41(12), 2337-2352.
- [6] A. Shaban, Gy. Vastag, and L. Nyikos, Piezogravimetric investigation of heterocyclic compounds as potential inhibitors against copper corrosion in acidic media, Int. J. Corros. Scale Inhib. 4(4), 2015, 328-337.
- [7] S. L. Cohen, V. A. Brusica, F. B. Kaufman, G. S. Frankel, S. Motakef, and B. Rush, X-ray photoelectron spectroscopy and ellipsometry studies of the electrochemically controlled adsorption of benzotriazole on copper surfaces, J. Vac. Sci. Technol. A, 8(3), 1990, 2417-2424.
- [8] K. F. Khaled, Corrosion control of copper in nitric acid solutions using some amino acids-a combined experimental and theoretical study, Corrosion Science, 52 (10), 2010, 3225-3234.
- [9] E. E. Oguzie, C. O. Akalezi, C. K. Enenebeaku, and J. N. Aneke, Corrosion inhibition and adsorption behaviour of malachite green dye on aluminium corrosion, chemical Engineering Communications, 198(1), 2011, 46-60.
- [10] J. Cruz, T. Pandiyan, and E. Garcia-Ochoa, A new inhibitor for mild carbon steel: electrochemical and DFT studies, Journal of Electroanalytical Chemistry, 583 (1), 2005, 8-16.
- [11] J. Cruz, R. Martinez, J. Genesca, and E. Garcia-Ochoa, Experimental and theoretical study of 1-(2-ethylamine-2-methylimidazoline as an inhibitor of carbon steel corrosion in acid media, Journal of Electroanalytical Chemistry, 566(1), 2004, 111-121.
- [12] E. E. Oguzie, Y. Li, S. G. Wang, understanding corrosion inhibition mechanisms-experimental and theoretical approach, RSC Advances, 1(5), 2011, 866-873.
- [13] I. Lukovits, K. Palfi, I. Bako, E. Kalman, Corrosion, LKP Model of the Inhibition Mechanism of Thiourea Compounds, Corrosion, 53(12), 1997, 915-919.
- [14] K. D. Sen, Electronegativity, Structure and Bonding 66, Springer Verlag, Berlin 1987.
- [15] K. D. Sen, Chemical hardness, Structure and Bonding 80, Springer Verlag, Berlin, 1993.
- [16] R. G. Parr and W. Yang, Density functional Theory of Atoms and Molecules, Oxford University Press, Oxford, U. K., 1989.

- [17] R. G. Parr and R. G. Pearson, Absolute hardness: Companion parameter to absolute electronegativity, *J. Am. Chem. Soc.*, 105(26), 1983, 7512-7516.
- [18] R. G. Parr and W. Yang, Density functional approach to frontier-electron Theory of chemical reactivity, *J. Am. Chem. Soc.*, 106(14), 1984, 4049-4050.
- [19] W. Yang and R. G. Parr, Hardness, Softness, and the Fukui function in the electronic Theory of metals and catalysis, *Proc. Natl. Acad. Sci. U. S. A.*, 82 (20), 1985, 6723-6726.
- [20] A. D. Becke, Density Functional thermochemistry. III. The role of exact exchange, *J. Chem. Phys.*, 98 (7), 1993, 5648-5652.
- [21] C. Lee, W. Yang and R. G. Parr, Development of the Colle Salvetti correlation-energy formula into a functional of the electron density, *Phys. Rev. B.*, 37 (2), 1988, 785-789.
- [22] B. Miehlich, A. Savin, H. Stoll and H. Preuss, Results obtained with the correlation energy density functionals of Becke and Lee, Yang and Parr, *Chem. Phys. Lett.*, 157 (3), 1989, 200-206.
- [23] S. G. Zhang, W. Lei, M. Z. Xia and F. Y. Wang, QSAR study on N-containing corrosion inhibitors: Quantum Chemical approach assisted by topological index, *Journal of Molecular Structure: THEOCHEM*, 732 (1-3), 2005, 173-182.
- [24] M. J. Frisch, G. W. Trucks, H. B. Schlegel et al., *Gaussian 03*, Gaussian, Inc.: Pittsburg P.A., 2003.
- [25] R. K. Dinnapa and S. M. Mayanna, Haloacetic Acid as Corrosion inhibitors for Brass in Nitric Acid, *Corrosion*, 38 (10), 1982, 525-530.
- [26] J. O' M. Bockris and D. A. J. Swinkels, Adsorption of n-Decylamine on Solid Metal Electrodes, *J. Electrochem. Soc.*, 111(6), 1964, 736-743.
- [27] P. Roy, P. Karfa, U. Adhikari and D. Sukul, Corrosion inhibition of mild steel in acidic medium by polyacrylamide grafted Guar gum with various grafting percentage: Effect of intermolecular synergism, 88, 2014, 246-253.
- [28] R. F. V. Villamil, P. Corio, J. C. Rubin, and S. M. L. Agostinho, Effect of sodium dodecylsulfate on Copper corrosion in sulphuric acid media in the absence and presence of benzotriazole, *J. Electroanal. Chem.*, 472 (2), 2011, 112-119.
- [29] S. Issadi, T. Douadi, A. Zouaoui, S. Chafaa, M. A. Khan and G. Bouet, Novel Thiophene symmetrical Schiff base compounds as corrosion inhibitor for mild steel in acidic media, *Corros. Sci.*, 53 (4), 2011, 1484-1488.
- [30] M. Belpour, S. M. Ghoreishi, N. Mohammadi and N. Salati-Niasari, Investigation of some Schiff base compounds containing disulphide bond as HCl corrosion inhibitors for mild steel, *Corros. Sci.*, 52 (12), 2010, 4046-4057.
- [31] N. M. Guan, L. Xueming and L. Fei, Synergistic inhibition between o-phenanthroline and chloride ion on cold rolled steel corrosion in phosphoric acid, *Mater. Chem. Phys.*, 86(1), 2004, 59-68.
- [32] A. Yurt, A. Balaban, S. U. Kandemir, G. Bereket and B. Erk, Investigation on some Schiff bases as HCl corrosion inhibitors for carbon steel, *Mater. Chem. Phys.*, 85(2-3), 2004, 420-426.
- [33] T. Koopmans, über die Zuordnung von wellenfunktionen und Eigenwerten Zuden Einzelnen Elektronen Eines Atoms, *Physica*, 1 (1-6), 1934, 104-113.
- [34] R. G. Parr, D. A. Donnelly, M. Levy and W.E. Palke, Electronegativity: The density functional viewpoint, *J. Chem. Phys.*, 68 (8), 1978, 3801-3807.
- [35] R. G. Pearson, Absolute electronegativity and hardness: application to inorganic chemistry, 27 (4), 1988, 734-740.
- [36] R. G. Parr, L. Von Szentpaly and S. Liu, Electrophilicity index, *J. Am. Chem. Soc.*, 121 (9), 1999, 1922-1924.
- [37] E. E. Ebenso, T. Arslan, F. Kandemirli, I. N. Caner, I. I. Love, Quantum Chemical Studies of some Rhodamine Azosulpha Drugs as corrosion inhibitors for mild steel in Acidic Medium, *International Journal of Quantum Chemistry*, 110, 2010, 1003-1018.
- [38] V. Hempriya, K. Parameswari and S. Chitra, Anticorrosion properties of benzothiazole derivatives for mild steel in 1 M H₂SO₄ Solution, *Chemical Science Review and Letters*, 3(12), 2014, 824-835.
- [40] B. Gomez, N. V. Likhanova, M. A. Dominguez-Aguilar, R. Vela, A. Martinez-Palou, J. Gasquez, Quantum Chemical Study of the Inhibitive Properties of 2-Pyridyl Azoles, *J. Phys. Chem. B* 110, 2006, 8928-8934.
- [41] P. Udhayakala, A. Maxwell Samuel, T. V. Rajendiran and S. Gunaseharan, DFT study on the adsorption mechanism of some Phenyltetrazole substituted compounds as effective corrosion inhibitors for mild steel, *Der Pharma Chemica*, 5(6), 2013, 111-124.
- [43] M. A. Quijano, M. Palomar-Pardavé, A. Cuan, M. R. Romo, G. N. Silva, R. A. Bustamante, A R. Lopez and H. H. Hernandez, Quantum Chemical Study of 2-Mercaptoimidazole, 2-Mercaptobenzimidazole 2-Mercapto-5-Nitrobenzimidazole as corrosion inhibitors for steel, *Int. J. Electrochem. Sci.*, 6(9), 2011, 3729-3742.